Chothia, C. (1974) *Nature 248*, 338-339.
Datta, S., Luo, C.-C., Li, W.-H., VanTuinen, P., Ledbetter, D. H., Brown, M. A., Chen, S.-H., Liu, S.-W., & Chan, L. (1988) *J. Biol. Chem. 263*, 1107-1110.
Derewenda, Z. S., & Helliwell, J. R. (1989) *J. Appl. Crystallogr. 22*, 123-137.
Derewenda, Z. S., & Cambillau, C. (1991) *J. Biol. Chem. 266*, 23112-23119.
Derewenda, Z. S., & Derewenda, U. (1991) *Biochem. Cell. Biol.* (in press).
Efimov, A. V. (1986) *Mol. Biol. (Moscow) 20*, 250-260.
Eisenberg, D., & McLachlan, A. D. (1985) *Nature 319*, 199-203.
Finkelstein, A., & Janin, J. (1989) *Protein Eng. 3*, 1-4.
Franken, S. M., Roseboom, H. J., Kalk, K. H., & Dijkstra, B. W. (1991) *EMBO J. 10*, 1297-1302.
Janin, J., & Chothia, C. (1990) *J. Biol. Chem. 265*, 16027-16030.
Jones, A. (1978) *J. Appl. Crystallogr. 11*, 268-272.
Joseph, D., Petsko, G. A., & Karplus, M. (1990) *Science 249*, 1425-1428.
Hendrickson, W. A. (1985) *Methods Enzymol. 115*, 252-270.
Honig, B. (1991) 15th International Congress of Biochemistry, Jerusalem, Collected Abstracts, p 123.
Howard, A. J., Gilliland, G. L., Finzel, B. C., Poulos, T. L., Ohlendorf, D. H., & Salemme, F. (1987) *J. Appl. Crystallogr. 20*, 383-387.
Huge-Jensen, B., Gailuzzo Rubano, D., & Jensen, R. G. (1987) *Lipids 22*, 559-565.
Kabsch, W., & Sander, C. (1983) *Biopolymers 22*, 2577-2637.
Leszczynski, J. F., & Rose, G. D. (1986) *Science 234*, 849-855.
Liao, D. I., & Remington, S. J. (1990) *J. Biol. Chem. 256*, 6528-6531.
Pathak, D., & Ollis, D. (1990) *J. Mol. Biol. 214*, 497-525.
Persson, B., Bengtsson-Olivecrona, G., Enerback, S., Olivecrona, T., & Jornval, H. (1989) *Eur. J. Biochem. 179*, 39-45.
Sarda, L., & Desnuelle, P. (1958) *Biochim. Biophys. Acta 30*, 513-521.
Schrag, J. D., Li, Y., Wu, S., & Cygler, M. (1991) *Nature 351*, 761-764.
Scott, D. L., Otwinowski, Z., Gelb, M., & Sigler, P. B. (1990a) *Science 250*, 1563-1566.
Scott, D. L., White, S. P., Otwinowski, Z., Yuan, W., Gelb, M. G., & Sigler, P. B. (1990b) *Science 250*, 1541-1546.
Sussman, J. L., Harel, M., Frolow, F., Oefner, C., Goldman, A., Toker, L., & Silman, I. (1991) *Science 253*, 872-879.
White, S. P., Scott, L. S., Otwinowski, Z., Gelb, M., & Sigler, P. B. (1990) *Science 250*, 1560-1563.
Winkler, F. K., D'Arcy, A., & Hunziker, W. (1990) *Nature 343*, 771-774.

Crystal Structure at 1.5-Å Resolution of d(CGCICICG), an Octanucleotide Containing Inosine, and Its Comparison with d(CGCG) and d(CGCGCG) Structures†,‡

Vinod D. Kumar,*,§ Robert W. Harrison,§ Lawrence C. Andrews,∥ and Irene T. Weber§

Macromolecular Structure Laboratory, National Cancer Institute, Frederick Cancer Research and Development Center, Advanced Biosciences Laboratories Basic Research Program, P.O. Box B, Frederick, Maryland 21702-1201, and Department of Pharmacology, Bluemle Life Sciences Building, Thomas Jefferson University, 233 South 10th Street, Philadelphia, Pennsylvania 19107

Received July 8, 1991; Revised Manuscript Received October 28, 1991

ABSTRACT: The octadeoxyribonucleotide d(CGCICICG) has been crystallized in space group $P6_522$ with unit cell dimensions of $a = b = 31.0$ Å and $c = 43.7$ Å, and X-ray diffraction data have been collected to 1.5-Å resolution. Precession photographs and the self-Patterson function indicate that 12 base pairs of Z-conformation DNA stack along the c-axis, and the double helices pack in a hexagonal array similar to that seen in other crystals of Z-DNA. The structure has been solved by both Patterson deconvolution and molecular replacement methods and refined in space group $P6_5$ to an R factor of 0.225 using 2503 unique reflections greater than $3.0\sigma(F)$. Comparison of the molecules within the hexagonal lattice with highly refined crystal structures of other Z-DNA reveals only minor conformational differences, most notably in the pucker of the deoxyribose of the purine residues. The DNA has multiple occupancy of C:I and C:G base pairs, and C:I base pairs adopt a conformation similar to that of C:G base pairs.

Inosine is a purine nucleoside whose neutral base forms stable base pairs with all four conventional bases, and the strength of the base pairing is approximately equal in each case (Martin et al., 1985). Inosine occurs naturally in the wobble position of the anticodon of some t-RNA's, where it appears to pair with adenosine in addition to cytidine and uridine, the nucleosides which pair with guanosine in that position. Poly(rI) and poly(dI) form stable helices with poly(rC) and poly(dC) (Felsenfeld & Miles, 1967) and serve as templates for the incorporation of cytosine into products of DNA and RNA polymerases (Hall et al., 1985). Oligonucleotides containing inosines have been used extensively as probes to screen human cDNA or genomic DNA libraries (Takahashi et al., 1985).

† This research was sponsored in part by the National Cancer Institute, DHHS, under Contract NO1-CO-74101 with ABL.

‡ The coordinates have been deposited in the Brookhaven Protein Data Bank (cgcicicg_dna.pdb).

* Author to whom correspondence should be addressed.

§ Present address: Department of Pharmacology, Bluemle Life Sciences Building, Thomas Jefferson University, 233 S. 10th St., Philadelphia, PA 19107.

∥ Present address: International Centre for Diffraction Data, 1601 Parklane, Swarthmore, PA 19081.

0006-2960/92/0431-1541$03.00/0

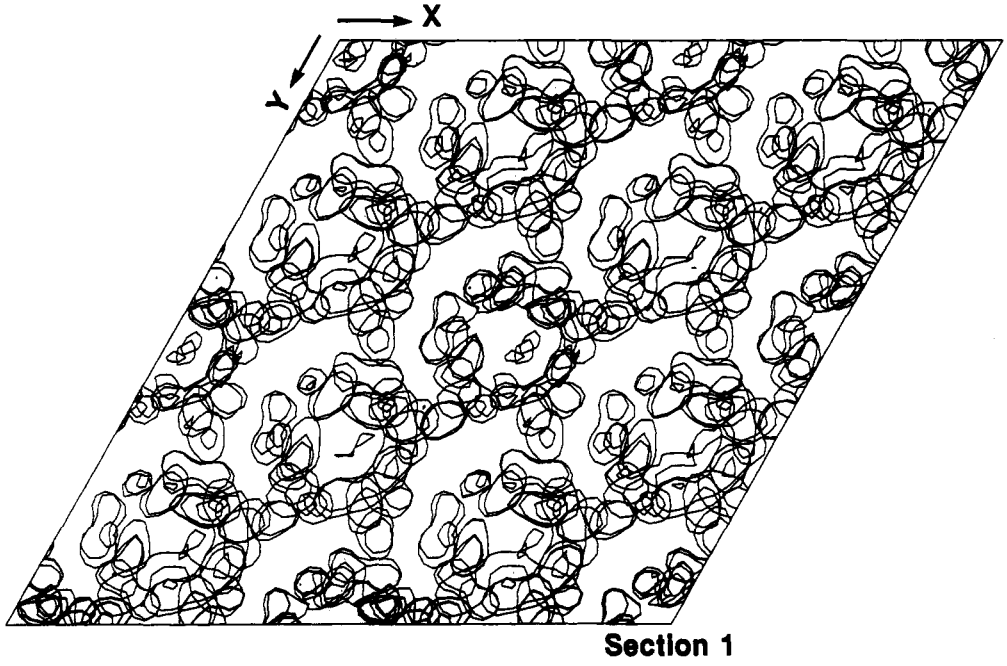

FIGURE 1: Electron density map calculated with phases from the Patterson deconvolution method and contoured at a level of 1.0σ. The view is down the z-axis, which is also the DNA helical axis, showing the hexagonal packing of the DNA helices in two unit cells.

These probes are generally used to reduce the degeneracy of pools of oligonucleotides, which has the advantage of reducing the possibility of mismatches and allowing the use of more stringent hybridization conditions.

Inosine is a purine nucleoside whose base, hypoxanthine, resembles guanine but lacks the 2-amino group. Base pairing between I and C is possible by forming two hydrogen-bond interactions, instead of the three that occur in C:G base pairs. Oligomers of alternating CG sequences have been shown to form left-handed helices in solution at high ionic strength (Pohl & Jovin, 1972) and in the crystalline state (Wang et al., 1979; Drew et al., 1980). Oligomers containing alternating pyrimidine–purine sequences have also been crystallized in the Z-DNA conformation, for example, the decadeoxyribonucleotide d(CGTACGTACG) (Brennan & Sundaralingam, 1985; Brennan et al., 1986). Other Z-DNA crystal structures include the modified bases, 5-methylcytosine (Fujii et al., 1982) or 5-bromocytosine (Chevrier et al., 1986). Previous studies using fiber diffraction have shown that poly(dI):poly(dC) formed B-DNA (Leslie et al., 1980). In contrast, circular dichroism spectra showed an unusual negative band at high wavelength for poly[d(I–C)]:poly[d(I–C)] which indicated a left-handed helical structure (Mitsui et al., 1970). Poly(dI:dC) showed different CD spectra than the left-handed Z-DNA, poly(dG:d5BrC), or the right-handed B-DNA form of poly(dG):poly(dC) (Fishel et al., 1990). In order to investigate the conformation of DNA containing I:C base pairs, oligomers containing C:I sequences were prepared and crystallized. We report here the first crystal structure of a Z-conformation DNA containing inosine–cytosine base pairs, and its comparison with the other published Z-DNA structures.

Materials and Methods

Synthesis, Crystallization, and Data Collection. The oligonucleotide d(CGCICICG) was synthesized by solid-phase phosphoramidite chemistry on an automated Applied Biosystems synthesizer, purified by ion-exchange liquid chromatography and reverse-phase high-pressure liquid chromatography, and assayed by polyacrylamide gel electrophoresis. Crystals were grown from a solution containing 2 mM DNA oligonucleotide, 1 mM spermine, 14 mM Mg acetate, and 20% 2-methyl-2,4-pentanediol, at room temperature by microvapor diffusion in the hanging drop method.

The space group and the unit cell dimensions of the crystals, which have the morphology of hexagonal rods, were determined by precession photographs. The symmetry of the $hk0$ plane and the systematic absences along 001 were consistent with space group $P6_522$ or the enantiomer $P6_122$. The unit cell dimensions of the crystals were $a = b = 31.0$ Å and $c = 43.7$ Å and $\gamma = 120°$. The crystals exhibited relatively large mosaic spread, suggesting internal crystalline disorder. The disorder is presumed to arise primarily from heterogeneity of individual molecules in the crystal lattice.

X-ray diffraction data were recorded to 1.5-Å resolution on a Siemens multiwire area detector mounted on a Rigaku RU-200 rotating anode generator, operated at 50 kV and 100 mA. A total of 9882 observations were measured and processed using XENGEN (Howard et al., 1987) in both space groups $P6_5$ and $P6_522$ to give 2949 and 1971 unique reflections, respectively. The data scaled to 0.076 and 0.081 internal agreement after rejection of outliers for the two respective space groups. Further tests showed that the agreement between hkl and khl reflections gave $R = 0.053$, which is indicative of the higher symmetry space group $P6_522$. Details of the statistics of the data processing in the space group $P6_522$ are summarized in Table I.

Determination of Structure. The precession photographs and detector data showed an intense 0,0,12 reflection at about 3.7-Å spacing in the $0kl$ plane. This is consistent with the position of the meridional reflection in fiber diffraction of Z-DNA that indicated a helical rise of 3.7 Å per base pair and suggested that the octamer is in the Z-DNA conformation.

The self-Patterson function (Patterson, 1952) was calculated in the z-projection and gave two peaks of 0.6 the height of the origin at ($^1/_3$,$^2/_3$), and ($^2/_3$,$^1/_3$) (Figure 1). The z-projection of the Patterson also showed four smaller peaks arranged symmetrically around each origin. This indicated the presence of two independent molecules in the asymmetric unit related by a translation of ($^1/_3$,$^2/_3$,0) or about 18-Å separation. This

Table I: Data Collection Statistics

resolution (Å)	no. of reflections possible	collected	no. of obs	fraction with $I > 1.5\sigma(I)$	R_{sym}[a]
10.00–2.80	400	375	2300	0.89	0.042
2.80–2.20	361	361	2179	0.94	0.074
2.20–1.92	348	348	1836	0.91	0.128
1.92–1.75	346	346	1639	0.90	0.205
1.75–1.62	334	319	1271	0.90	0.129
1.62–1.50	345	222	584	0.50	0.273
10.00–1.50	2134	1971	9809	0.84	0.081

[a] $R_{sym} = \sum_h\sum_i|\langle I\rangle - I(h)_i|/\sum_h\sum_i I(h)_i$ for symmetry-related observations.

and the six peaks in the Patterson in the y–z plane show the packing of 12 base pairs of double helix along the z-axis with 3.7-Å separation between base pairs and internal 6-fold symmetry. The asymmetric unit would be a dimer (two base strand) repeated around a 6-fold screw axis to make a helix with 12 base pairs per turn and a tetramer (four base strand) on a 3-fold screw axis with every fourth phosphate missing to give rise to a 12-fold helix. It has to be noted that although the actual molecule is an octamer DNA d(CGCICICG), the asymmetric unit consists of degenerate parts of this DNA on the 3-fold and 6-fold screw axes. These degenerate parts are referred to as dimer and tetramer. In addition, this kind of disorder structure results in a packing where the purine residues (guanine and inosine) in the asymmetric unit overlap and are therefore referred to as G(I). The unit cell dimensions and Patterson maps indicated that d(CGCICICG) DNA crystallized in the same hexagonal lattice as the parent DNA, d(CGCGCGCG) (Fuji et al., 1985). Since the coordinates for d(CGCGCGCG) DNA were not available, we have solved the crystal structure of d(CGCICICG) DNA by two independent methods: (a) Patterson deconvolution and (b) molecular replacement.

Patterson Deconvolution. The Patterson deconvolution method (Harrison, 1990) was applied to give an independent solution of the packing and molecular structure. The structure was solved by a direct inversion of the Patterson function, a new method described in Harrison (1990). This approach is based on the observation that the Patterson function is a quadratic function of the electron density values. This is not obvious from the classical structure factor formula for the Patterson, $\sum I_{obs} \cos(2\pi hx)$, but stems from the fact that the equations for the self-convolution are quadratic when written out for the individual map grid points. Because of this underlying simplicity, it is possible to construct numerical methods for the solution of the Patterson function (its deconvolution). A large number of numerical optimization methods, including but not limited to conjugate gradients, steepest descents, fixed point iteration, simulated annealing, simplex, and relaxation methods, will solve Patterson functions with varying degrees of efficiency. Independent of the optimizer used, a bounded electron density is found that reproduces the observed Patterson function. In this case, because of the high degree of crystal symmetry in $P6_522$, a relaxation algorithm over the space of the phase variable was chosen. The reason for choosing a relaxation algorithm is that the centric phases are restricted by crystal symmetry, and since there are many centrics in this space group, systematically choosing such phases is more efficient. Starting from the most intense reflections, and gradually including the weaker reflections, the phase of each reflection was varied over its complete range and the phase with the lowest error upon truncation was chosen. This is an iterative relaxation algorithm and requires several passes for convergence.

In order to make the evaluation of the error in the Patterson function more efficient (since it is calculated a large number of times), precalculation was used wherever possible to increase the speed. In order to do this, a copy of the prior map excluding the components of the reflection being searched was made. The complete map with all the reflections is quickly generated by adding the Fourier terms for the omitted reflections. The error was evaluated as the integral over the unit cell of the square of the difference between the prior map and the complete map, with the prior map truncated to reflect the previous bounds of the electron density. This is not exactly the same as the square error of Harrison (1990), but it has the same zeros and similar convergence properties. This measure is the sum of the difference between a map which has a correct Patterson (by definition as it has only observed Fourier coefficients) and one which meets the bounds on the electron density. If we use the square error, then, by Parseval's theorem when this difference is minimal, the difference in the Fourier coefficients and the Pattersons is minimal as well.

The initial electron density map is shown in Figure 1. The initial model building was carried out in both space groups $P6_522$ and $P6_122$ using ideal Z-DNA. This direct solution was more consistent with space group $P6_522$, since, if the calculation was run in space group $P6_122$, the electron density resembled right-handed Z-DNA. The Z-DNA coordinates were positioned in the initial electron density map, and the solution was rapidly refined in space group $P6_522$ using XPLOR (Brunger, 1988) to an R factor of 0.25 with 2.5-Å resolution data. This showed that the crystal consists of disordered helices of Z-DNA with the helical axis along the z-direction and packed in a hexagonal array at about 18-Å helix–helix separation. When the structure refinement was continued (after comparison with the initial molecular replacement model showed that the structures were the same), the symmetry was reduced to $P6_5$ in case the disorder at the inosines was only a pseudo-22 symmetry and to make the enforcement of intramolecular hydrogen-bond geometry simpler.

Molecular Replacement. The structure was determined by molecular replacement in space group $P6_522$ using ideal Z-DNA as a starting model. The hexagonal lattice has sites with 6-fold and 3-fold screw symmetry. The relative position and orientation of each helix was determined with a four base Z-DNA model by the molecular replacement method using the programs MERLOT (Fitzgerald, 1988) and XPLOR (Brunger, 1988). The rotation function search was conducted using data from 8- to 3.0-Å resolution. These searches gave two strong symmetry-related rotation function peaks with intensities above 75% of the maximum. Next, the R value was calculated at 0.25-Å intervals for translations along the z-axis for the four base Z-DNA molecule positioned on the 3-fold screw axis ($^1/_3$,$^2/_3$,0). This molecule was fixed at the position indicated by the minimum. The two base Z-DNA molecule was then centered on the 6-fold screw axis (0,0,0), rotated every 5°, and translated at 0.25-Å intervals along the z-axis to find the position of minimum R factor. The final R factor after the model building was 0.52 for 8–3.5-Å resolution using 285 of the strongest reflections with structure factor amplitudes (F) greater than 2σ.

Refinement. For the refinement, the space group of the crystal was lowered to $P6_5$. The asymmetric unit consisted of a two base pair Z-DNA molecule on the 6-fold screw axis and a three base pair Z-DNA molecule on the 3-fold screw axis. This procedure enabled the introduction of base-pair hydrogen-bonding restraints. The bases are labeled C1 through G(I)2 in the 5′ to 3′ direction on strand 1, and C11

Table II: Summary of the Refinement Statistics

resolution (Å)	no. of reflections obsd[a]	no. of reflections percent[b]	*R* factor[c]
5.00–3.50	184	87	0.104
3.50–3.00	155	87	0.137
3.00–2.80	101	88	0.186
2.80–2.50	206	84	2.09
2.50–2.30	196	81	0.235
2.30–2.10	266	80	0.312
2.10–2.00	169	75	0.370
2.00–1.90	199	73	0.320
1.90–1.80	241	71	0.290
1.80–1.70	324	76	0.332
1.70–1.60	324	61	0.335
1.60–1.50	138	30	0.380
5.00–1.50	2503	71	0.225

[a] The number of reflections indicated in this column is for the expanded data set for the lower symmetry space group $P6_5$ with reflections $F > 3\sigma$. [b] Percent of the total possible reflections in the shell. [c] $R = \sum_h ||F_o| - |F_c|| / \sum_h |F_o|$.

Table III: Refinement Parameters

R factor	0.225
weights	$w = \sigma_F^{-2}$
with	$\sigma_F = (1.3) + (-1.7) \times [s - (1/6)]$
resolution range (Å)	5.0–1.5
no. of reflections	2503
no. of atoms	305
distance restraints[a]	
sugar–base bond distances	0.027 (0.025) Å
sugar–base angle distances	0.064 (0.050) Å
phosphate bond distances	0.083 (0.050) Å
phosphate bond angle distances	0.111 (0.075) Å
plane restraints[a]	0.042 (0.030) Å
chiral center restraints[a]	0.114 (0.100) Å^3
nonbonded restraints[a]	
single-torsion contact	0.251 (0.250) Å
multiple-torsion contact	0.453 (0.250) Å
B_{iso} restraints[a]	
sugar–base bonds	7.140 (5.000) Å^2
sugar–base angles	8.573 (7.500) Å^2
phosphate bonds	8.732 (7.500) Å^2
phosphate bond angles	8.350 (7.500) Å^2

[a] rms deviations from ideality (target restraints in parentheses).

through G(I)12 on strand 2, for the two base pair molecule around a 6-fold screw axes. The bases for the four base pair molecule around the 3-fold screw axes are numbered from C4 through G(I)7 on strand 1 and C17 through G(I)20 on strand 2. The molecular replacement solution was initially refined by a six-dimensional rigid body method to an *R* factor of 0.40–4.0-Å resolution, using XPLOR. At this stage, Fourier sum ($2F_o - F_c$) and difference maps ($F_o - F_c$) were displayed on an Evans and Sutherland PS390 graphics terminal with the program FRODO (Jones, 1985). The electron density was nearly continuous around the DNA backbone and bases. Refinement was carried out independently using both the refinement packages XPLOR (Brunger, 1988) and NUCLSQ (Westhoff, 1985). The refinement was extended to 1.5 Å in several stages. At each stage, a series of Fourier sum and difference maps were calculated and displayed on the graphics terminal. Manual intervention was required during each of these stages to adjust the model to fit the electron density. After refinement to 2.2 Å, series of difference Fourier maps was calculated at each stage and a peak search program was used to locate water molecules. The criteria for selection of solvent molecules were (1) the location of a spherical peak in the difference Fourier map greater than 2.5 standard deviations in height; (2) potential hydrogen-bonding partners within 2.2 to 3.3 Å; and (3) an acceptable thermal parameter of less than 50 Å^2 obtained after subsequent refinement. All solvent peaks were represented as water molecules, since it was not possible to specifically identify sodium, magnesium, or spermine ions. The overall *R* factor for the final model including 58 solvent water molecules is 0.225 at 1.5-Å resolution for 2503 reflections with $F > 3.0\sigma(F)$. The details concerning diffraction data and refinement parameters are summarized in Tables II and III, respectively.

Results and Discussion

The structure was solved by a combination of techniques. Examination of the unit cell and Patterson synthesis indicated the packing arrangement and suggested the presence of Z-DNA. The Patterson deconvolution method gave a direct determination of the phases and showed that the structure was Z-DNA in space group $P6_522$, rather than $P6_122$. This is the second large DNA crystal structure to be directly phased. The first was d(CGCGAAATTTACGCG) with two unpaired bases (Miller et al., 1988), which was solved by a minimum cross entropy method (Harrison, 1989). This illustrates the utility of direct phasing techniques for rapidly solving DNA structures in nonisomorphous crystals or when the presence of several molecules in the asymmetric unit makes molecular replacement more difficult. Finally, the d(CGCICICG) structure was independently solved by molecular replacement in several stages.

Helix Structure. This structure was refined as an alternating CG, although the crystal actually contains d(CGCICICG) with 0.5 occupancy of G and I at the purines. The regular packing into a hexagonal arrangement of Z-DNA double helices at about 18-Å helix–helix separation is typical of crystal structures of other oligomers of Z-DNA (Wang & Rich, 1985). The first Z-DNA structure of d(CGCGCG) crystallized in space group $P2_12_12_1$, but the packing of molecules is pseudohexagonal. As mentioned earlier, a very similar packing of Z-DNA helices is seen in the structures of disordered sequences, d(CGCGCGCG) and d(CGTACGTACG), which have been determined in space group $P6_5$ (Fuji et al., 1985). The crystal structure of d(CGCICICG) described here shows a similar hexagonal packing in space group $P6_522$. The asymmetric unit consists of two independent DNA molecules: a dimer two base strand) at the 6-fold screw axes and a tetramer (four base strand) at the 3-fold screw axes. The root mean square (rms) differences after a least-squares superposition for all atoms between these two independent molecules is 0.55 Å. The differences between these molecules on the 6-fold and 3-fold positions are minor and arise from the fact they are independent molecules, i.e., they are not constrained to be identical by any lattice symmetry (Crawford et al., 1980). It is important to note that the asymmetric contents will now be referred to as a two base pair strand and a four base pair strand (found in the lower space group $P6_5$ rather than the two base and four base strands present in $P6_522$.

Figure 2 shows a stereo side view of the packing of three duplex molecules of the tetramer on the 3-fold screw axes. As with the d(CGCG) or d(CGCGCG) Z-DNA structures, this molecule has only one deep groove, which is analogous to the minor groove of B-DNA. The stands from each of these molecules form a continuous helix with its chemically equivalent self-complementary strand along the *c*-axis. We have compared the structure of d(CGCICICG) with the refined crystal structures of the d(CGCGCG) Z-DNA (Gessener, 1989) and d(CGCG) Z′-DNA (Drew, 1980). The overall conformation of the inosine-substituted d(CGCICICG) oc-

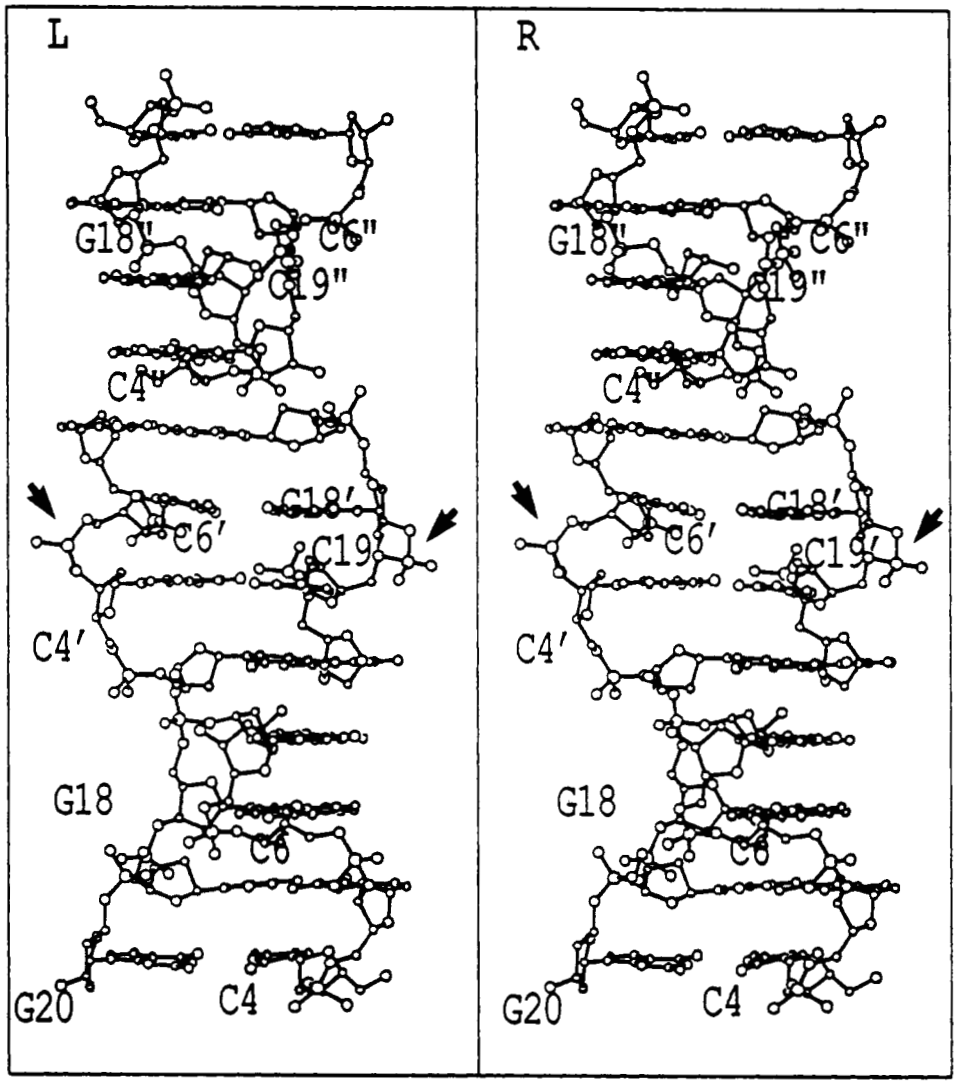

FIGURE 2: Stereodiagram showing packing of three duplex molecules of the tetramer located on the 3-fold screw axes. The molecules are stacked along the *c*-axis of the crystal and form a continuous double helix. The phosphate groups of the central G(I)pC steps reveal two separate orientations Z_I and Z_{II}, which are indicated by arrows. The phosphate between G5′ and C6′ on strand 1 is rotated away from the groove in Z_{II} conformation, and the phosphate between G(I)18′ and C19′ is rotated toward the groove in the helix in Z_I conformation.

tamer is similar to that of the other known Z-DNA structures. The root mean square (rms) differences after a least-squares superposition between all equivalent atoms is 0.61 Å for both d(CGCG) and d(CGCGCG) DNA molecules. However, the differences between these structures are not associated with differences in the stacking of base, i.e., the stacking of CpG(I) and G(I)pC sequences is virtually identical to those reported for the other two structures. The differences between d(CGCICICG) and d(CGCGCG) structures are primarily confined to the phosphate groups, but, with d(CGCG) DNA, the differences are found over the rest of molecule as well. Figure 3a,b presents the C:G(I) base pairs and their associated solvent structure superimposed on the electron density map $(2F_o - F_c)$. The base pairing between the cytosine and inosine is of the Watson–Crick type, in an antiparallel helix. The angles between the glycosyl bond and the C1′···C1′ vector for the base pairs are well within the narrow range of 52°–62° observed for Watson–Crick base pairs (Kennard, 1988), suggesting no wobble base pairing between inosine and cytosine.

Base Stacking. Table IV lists a comparison of various helical parameters for the three DNA structures based on the IUPAC-IUB nomenclature (1989). Although the backbone is minimally perturbed by substituting guanosine with inosine, there are variations in the local geometry of the bases. The tip angle, which defines the rotation of the base pair plane about the long helix of the base pair perpendicular to the helix axis, shows a high value for the terminal base pairs, for both the d(CGCG) and d(CGCGCG) structures. In contrast, the d(CGCICICG) structure shows a high value only for the central base pair steps. The roll angles display an alternation for the d(CGCG) structure with a low value for the GpC step and a high value for the CpG step, consistent with Calladine's rules (Calladine, 1982) for an alternating sequence. However, the d(CGCGCG) and d(CGCICICG) structures show lower values for CpG(I) than G(I)pC steps. This alternation is the reverse of the expected order. The average inclination angles for the d(CGCGCG) and d(CGCICICG) structures are lower (−4.3 and −4.7) than that of the d(CGCG) structure (2.2). The propeller twist and buckle are the dihedral angles formed between the individual bases when viewed along the long and short axis respectively. The d(CGCGCG) structure exhibits the characteristic negative propeller twist at all the base pairs, whereas the d(CGCG) and d(CGCICICG) structures show negative propeller twists only for the G(I)pC steps. The buckle angle, which is another measure of the noncoplanarity, is significantly different for all three structures. However, these values for the individual base pairs in d(CGCICICG) and

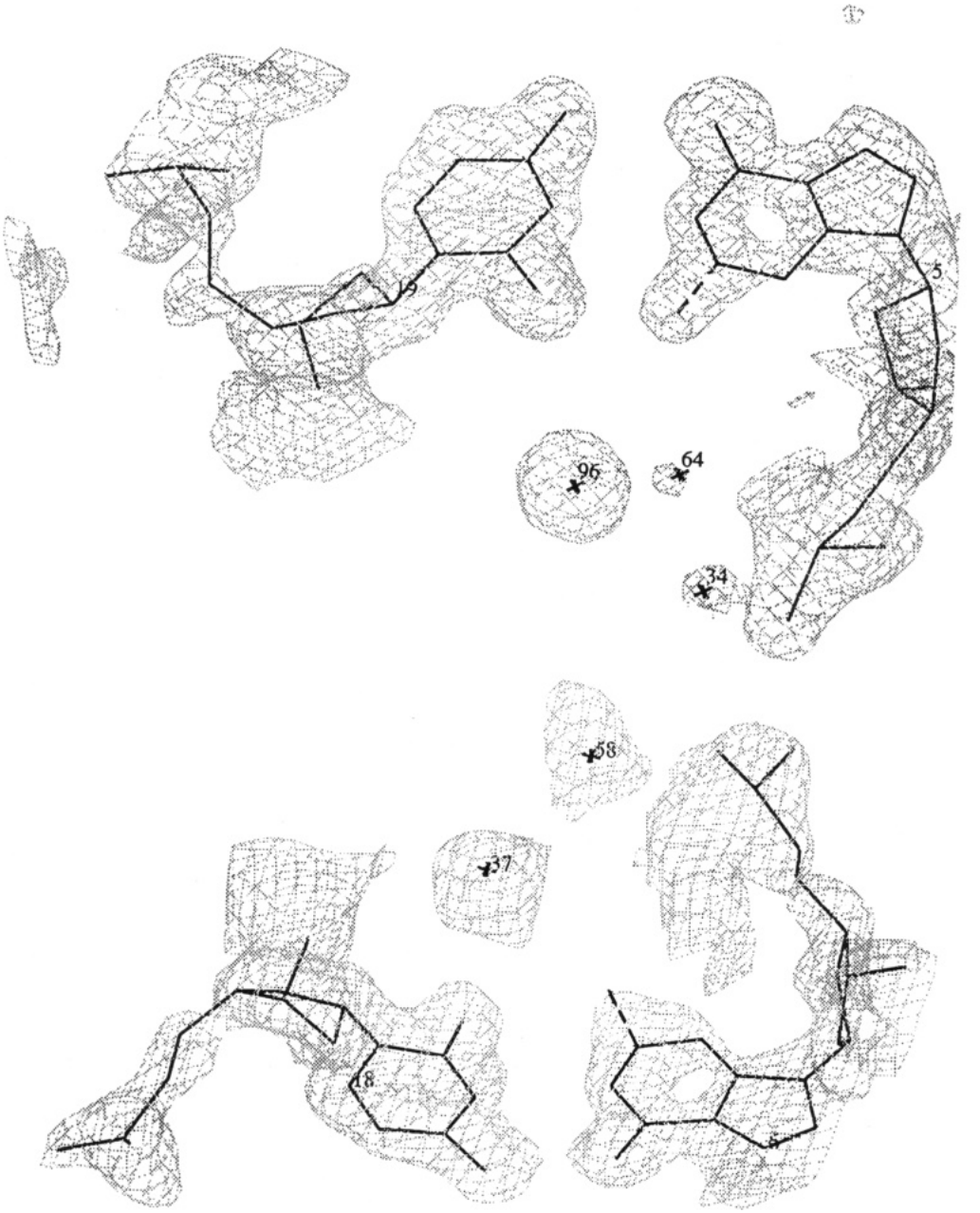

FIGURE 3: C:G(I) base pair and its solvent structure superimposed on a section of a $2F_o - F_c$ electron density map calculated after refinement of the structure at 1.5-Å resolution. The electron density is contoured at a level of 1.0σ and is shown in dashed lines, while the atomic coordinates are indicated by continuous lines. The bonds connecting C2 and N2 are also indicated as dashed lines. (a, top) C19:G(I)5; (b, bottom) C6:G(I)18.

d(CGCG) do follow the same trend but are larger in magnitude than in the d(CGCGCG) structure. The C:G(I) base pairs show positive buckle, while G(I):C base pairs show negative buckle angles. The average buckle angle for d(CGCICICG) DNA is higher than that of the two structures. These high values may be a consequence of optimizing the stacking interactions with the sugar–phosphate backbone of other symmetry-related molecules and/or due to the different crystal lattice forces. The octamer d(CGCICICG) adopts a double-helical structure with a helical twist of −60° for one dinucleotide repeat. However, there is a major difference in the twist angles for the CpG(I) or G(I)pC steps. For the d(CGCGCG) molecule, the twist angle for the CpG pair is −8°, compared to a significantly larger rotation of −51° for the GpC base pair. The twist angles for the d(CGCICICG) DNA are slightly changed, the CpG(I) is increased to −17°, while the G(I)pC angle has correspondingly changed to −43°. A similar observation is seen with d(CGCG) structure. The net effect of these changes in the twist angle is to bring the cytosine groups closer to the guanine (inosine) residues (Drew, 1980). The DNA molecule along the 6-fold screw axes has twist angles similar to those of the d(CGCGCG) molecule, i.e., the twist angles are −10° and −50° for the CpG(I) and G(I)pC steps, respectively. The *x*-displacement values show significant variations in the hexagonal structure d(CGCGCG), with lower values for the central base pair steps. In contrast, the d(CGCG) and d(CGCICICG) structures show uniform *x*-displacement for all base pair steps.

Backbone Conformation. Table V lists a comparison of the sugar–phosphate backbone and glycosidic torsion angles for the three DNA structures. The average glycosidic torsion angle χ for the pyrimidine residues is 189°, which is slightly different from that of the d(CGCG) DNA (200°) and d(CGCGCG) DNA (209°) but still consistent with the anti conformation. The purine residues adopt a syn conformation; the average χ angle is 71° compared to 70° and 65° for

Table IV: Helical Parameters[a] of d(CGCICICG),[b] d(CGCG),[c] and d(CGCGCG)[d] DNA Structures

sequence	tip	inclination	roll	propeller twist	buckle	twist	rise	x-disp
C	2.4	4.0	−2.6	0.3	−9.4	16.5	3.6	−3.3
	8.8	2.3	−8.0	−0.7	−7.2	12.8	3.8	−3.4
	6.6	5.6	5.3	−0.2	−2.5	7.3	3.8	−3.0
G(I)	−0.1	5.1	4.9	2.1	7.7	43.5	3.7	−3.2
	0.8	−3.0	−1.3	−1.4	7.6	44.7	3.7	−2.9
	2.0	4.2	3.5	−3.9	4.4	50.4	3.8	−2.6
C	4.8	4.8	−2.9	2.7	−10.1	16.4	3.7	−3.1
	−0.5	−2.3	−10.7	3.7	−8.3	14.2	3.7	−3.0
	1.2	2.7	4.1	−1.8	−4.5	7.7	3.6	−1.6
G(I)	1.9	5.1	–	−0.8	3.3	–	–	−3.1
	−2.3	3.7	1.7	−0.1	4.5	51.8	3.6	−1.6
C	–	–	–	–	–	–	–	–
	–	–	–	–	–	–	–	–
	−0.4	4.4	2.3	−0.7	−3.3	10.7	3.8	−2.7
G	–	–	–	–	–	–	–	–
	–	–	–	–	–	–	–	–
	−1.6	5.3	–	−2.3	0.1	–	–	−3.1
mean	2.2	4.7	−0.2	1.1	−2.1	26.0	3.6	−3.2
	−0.5	2.2	−6.7	−0.61	−1.2	24.0	3.8	−3.2
	0.9	4.3	3.4	−1.5	−0.2	25.6	3.7	−2.4

[a] Helical parameters were calculated with program NEWHELIX91 distributed by R. E. Dickerson. [b] Parameters were determined for only the tetramer on the 3-fold screw axis. [c] Parameters for d(CGCG) DNA (Drew et al., 1980) are given on the second line. [d] Parameters for d(CGCGCG) DNA (Gessener et al., 1989) are given on the third line. All value are given in degrees except rise and x-displacement, which are in angstrom units. the values of inclination and x-displacement should be reversed for Z-DNA.

d(CGCG) and d(CGCGCG) structures, respectively. The average glycosidic torsion angle χ for the molecule on the 6-fold screw axis agrees quite well with the χ angles of other Z-DNA structures. The two strands of the inosine-containing d(CGCICICG) DNA form an antiparallel left-handed double helix in which the purine (guanine and inosine) residues are in syn conformation and the pyrimidine (cytosine) residues are in anti conformation.

The average pseudorotation phase angle of deoxyribose rings of the pyrimidine residues for the molecule (tetramer) on the 3-fold screw axes is 160°, typical of a C2′-endo pucker, while the corresponding average pseudorotation angle for the purine residues is 110°, which is typical of a C1′-exo conformation. However in the d(CGCGCG) DNA structure, the deoxyribose rings of pyrimidine residues take up a C2′-endo pucker while the purine residues assume a C3′-endo puckering conformation. The average pseudorotation angles of deoxyribose rings of the pyrimidine residues for the molecule (dimer) on the 6-fold screw axes are in C2′-endo conformation (155°), while purine residues assume a C3′-endo conformation (65°). The sugar–phosphate backbone (δ) torsion angles, which are often a better guide to sugar puckering, agree well with the average pseudorotation angle. For instance, the average δ angles for pyrimidines for the tetramer are 141°, indicating that they are in C2′-endo conformation, and 116° for purines residues, which are in C1′-exo conformation (Levitt & Warshel, 1978).

The C1′-exo conformation (variant of the C2′-endo) was first observed in the tetramer d(CGCG) (Drew, 1980) and is now termed Z′-DNA. This sugar pucker can be regarded as a slightly bent C2′-endo form, and the variation is a result of a relatively short intramolecular contact between the N3 nitrogen atom in a guanine or inosine ring and the C2′ atom in the sugar ring that is in a syn orientation relative to the base. In contrast, if the sugar pucker was in a C2′-endo conformation, this would push the N3···C2′ atoms closer together, thus leading to an unacceptably short nonbonded contact. In the d(CGCGCG) structure, the sugars adopt C3′-endo puckering to avoid the shorter nonbonded contact. The P···P distances range from 5.4 to 8.3 Å, with an average of 6.6 Å. The average P···P values for d(CGCG) and d(CGCGCG) DNA are 6.7 and 7.2 Å, respectively. The phosphate groups of GpC are found in two conformations in Z-DNA (Wang et al., 1981). These two conformations have been called Z_I and Z_{II}, respectively; conformation Z_I is synclical(−), gauche(−)–trans for the phosphodiester conformation, while Z_{II} is synclical(+), gauche(+)–trans. In the present structure, two G(I)pC sequences are found, both associated with the molecules at the 3-fold screw axes. In this molecule, the phosphate linking G(I)5 and C6 in strand 1 (Figure 2) is rotated toward the center of the groove in Z_I position. For this conformation the, ζ of G(I)5 is in the −sc conformation, while the phosphate linking G(I)18 and C19 in strand 2 is rotated downward away from the groove in the Z_{II} position. The corresponding ζ angle of G(I)18 is in +sc conformation. The crystal packing for the d(CGCICICG) structure is shown in two views in Figure 4a,b. There are two intermolecular contacts between the molecules on the 6-fold screw axes and the molecules lying along the 3-fold screw axes: N7 atom of G(I)-2 with O1P atom of C-17, and O3′ atom of G(I)-5 and O2P atom of G(I)-12. The switch of the sugar pucker of G(I) residues from C3′-endo to C1′-exo not only affects the local base parameters but also perturbs the neighboring base pairs. It is very likely that this distortion is brought about by crystal packing. If G(I) bases were to adopt the standard C3′-endo sugar pucker, there would be clashes with the neighboring molecules.

Thermal Motions and Solvent Structure. The isotropic temperature factors (*B* factors) reflect the mobility of the atoms within the crystal. The average thermal parameters of the bases (15.4 Å^2) are lower than those of sugars (24 Å^2) or phosphate groups (33 Å^2), reflecting a lesser mobility for the bases. In the course of refining the structure of d(CGCICICG) to 1.5-Å resolution, 58 solvent molecules were located, compared to 85 solvent molecules reported for the Z-DNA structure d(CGCGCGCG) (Fuji, 1985). The lower number of water molecules probably reflects more conservative criteria for locating the solvent molecules. The solvent thermal parameters range from 23 to 47 Å^2. Two well-defined water molecules were observed in the minor groove of the d[C:G(I)] base pair, consistent with what has been observed in the minor groove cervices of the d(C:G) base pairs in all of the Z-DNA

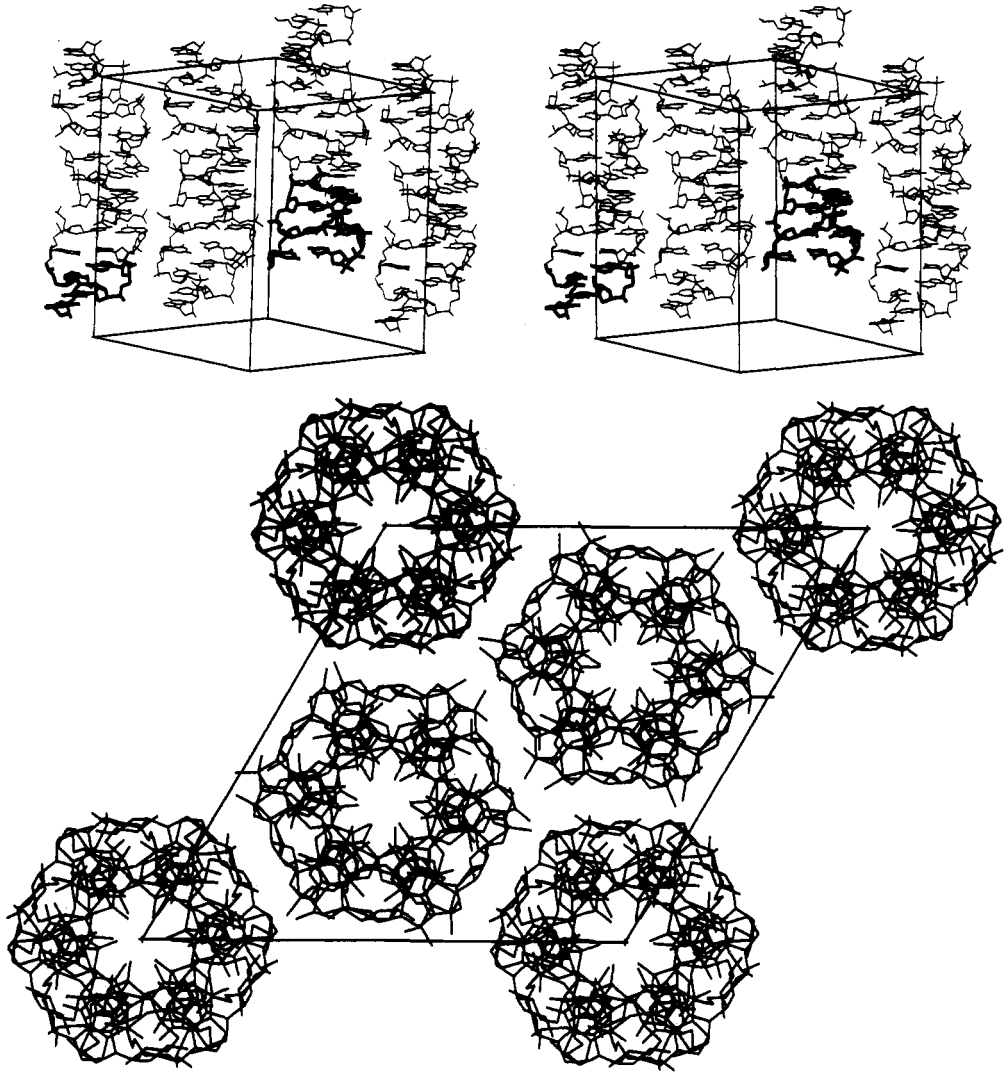

FIGURE 4: (a, top) Stereoview of the crystal packing for d(CGCICICG) structure looking down the *a*-axis. The molecules found at the corners of the unit cell have 6_1 or 6_5 symmetry, whereas the internal molecules have 3_1 symmetry. The contents of the asymmetric unit in the space group $P6_5$ (two base pair on the 6-fold screw axes and four base pair on the 3-fold screw axes) are displayed in darker lines. (b, bottom) View down the *c*-axis of the crystal structure.

structures studied so far. These waters form a continuous spine along the minor groove in the case of the d(CGCGCG) structure, which is thought to be important for stabilizing Z-DNA in this structure. A total of 41 of the solvent molecules are involved in intermolecular contacts, of which 17 contact symmetry-related molecules. The N-4 atom of the 5′ cytosines and the N-7 atom of 3′ guanines or inosines forms contacts with water. Most of the phosphate anionic oxygens are involved in hydrogen bonds and are individually hydrated. Five solvent molecules are involved in bidentate intraphosphate interactions between a phosphodiester oxygen O5′ and a free phosphate oxygen. In addition, there are four water molecules that interact with two free phosphate oxygens of the same phosphate group. The deoxyguanosine(inosine) in the central base pair steps are stabilized in syn conformation by water molecules bridging the N2 and a phosphate oxygen atom. The missing phosphate between O3′ of G(I)-7 (molecule 1) and O5′ of C-4 (molecule 2) is mimicked by a solvent molecule connecting both oxygen atoms by hydrogen bonds. This interstrand stacking has resulted in a slight rotation around the O5′–C5′ (β) bond of G(I)-5 and G(I)-7, resulting in change in α from a standard +sc (63°) to −sc (301°) and a change in γ from ap (178°) to −sc (326°).

Conclusions. The determination of the crystal structure of d(CGCICICG) was unusual in that it was independently solved by two techniques: a direct phasing by the Patterson deconvolution method and molecular replacement using the Z-DNA d(CGCGCG). The present analysis establishes that the octamer duplex d(CGCICICG), like the parent d(CGCGCGCG), forms a Z-type structure under the crystallization conditions employed. A comparison of the inosine-containing d(CGCICICG) DNA molecule with the two other Z-DNA structures reveals minor differences in the helical parameters and backbone. The crystal structure of d(CGCICICG) shows that inosine can replace guanine and still retain the conformation of the parent DNA. The most striking aspect of the Z-DNA molecules is the virtual identity of the corresponding base steps in all three helices, even though they were crystallized under different conditions and their crystal structures were refined independently. Although all three structures have a fundamental similarity in that the base pairs stack in an identical manner, the packing interactions are quite different in all three crystal forms. In the three structures, the base pairs differ in hydration, thermal parameters, and base stacking interactions. Many of these differences in the three crystal forms can be explained by the packing interactions, which are responsible for distortions of the duplexes at different locations (Jain & Sundarlingam, 1989).

Table V: Sugar–Phosphate Backbone, Glycosidic Torsion Angles, and Pseudorotation Phase Angles (P)[a] of d(CGCICICG),[b] d(CGCG),[c] and d(CGCGCG)[d] DNA Structures

	sequence							
strand 1	α	β	γ	δ	ϵ	ζ	χ	P
C-4	–	–	204	158	274	104	183	183
	–	–	239	138	282	78	193	154
C-1	–	–	52	145	265	79	210	154
G(I)-5	296	176	321	139	202	308	92	141
	86	170	165	116	240	303	64	110
G-2	61	188	178	91	240	295	60	40
C-6	109	205	117	144	276	97	181	165
	178	205	87	137	261	87	182	137
C-3	212	239	50	148	260	81	210	145
G(I)-7	307	154	331	111	–	–	86	88
	41	193	200	103	–	–	64	−22
G-4	64	186	179	92	181	69	59	26
	–	–	–	–	–	–	–	–
	–	–	–	–	–	–	–	–
C-5	166	160	48	142	260	80	208	151
	–	–	–	–	–	–	–	–
	–	–	–	–	–	–	–	–
G-6	76	175	182	149	–	–	78	170

	sequence							
strand 2	α	β	γ	δ	ϵ	ζ	χ	P
C-17	–	–	68	128	269	71	195	134
	–	–	27	140	268	72	214	160
C-7	–	–	55	139	268	74	209	157
G(I)-18	96	183	170	108	201	45	60	111
	76	175	179	120	181	25	75	128
G-8	67	189	172	101	236	335	61	36
C-19	186	136	42	136	250	87	196	158
	175	182	39	148	289	47	210	162
C-9	198	196	55	140	268	74	205	153
G(I)-20	89	191	177	105	–	–	58	100
	96	163	184	148	–	–	77	173
G-10	64	185	179	96	244	290	62	35
	–	–	–	–	–	–	–	–
	–	–	–	–	–	–	–	–
C-11	210	241	56	142	259	70	204	151
	–	–	–	–	–	–	–	–
	–	–	–	–	–	–	–	–
G-12	84	183	183	149	–	–	72	162

[a] Glycosidic torsion angles and pseudorotation phase angles were calculated with program NEWHELIX91 distributed by R. E. Dickersen. [b] Parameters were determined for only the tetramer on the 3-fold screw axis. [c] Parameters for d(CGCG) DNA (Drew et al., 1980) are given on the second line. [d] Parameters for D(CGCGCG) DNA (Gessener et al., 1989) are given on the third line.

The most noteworthy features of the inosine-containing DNA structure are that the base pairing between cytosine and inosine is of the Watson–Crick type and the sugar puckering for the purines are of the C1′-exo type. The torsion angles α and γ of G(I)-5 and G(I)-7 undergo a crankshaft rotation, which is not observed in the two other reference helices d(CGCG) and d(CGCGCG). This motion in the backbone is a result of the interbase contacts. These observations suggest that substitution of inosine has very little effect on the overall conformation of the Z-DNA. The minor differences in the sugar puckering and backbone are probably a direct result of crystal packing and not a result of the base substitution.

Acknowledgments

We are grateful to Richard Fishel for the suggestion of using inosine. We thank Dr. M. Gribskov for helpful discussions, M. Powers for synthesizing oligonucleotide, and Dr. R. E. Dickerson for providing us with the NEWHEL91 program. Part of this research was sponsored by the National Cancer Institute, DHHS, under Contract No. N01-C01-74101 with ABL. The contents of this publication do not necessarily reflect the views or policies of the Department of Health and Human Services, nor does mention of trade names, commercial products, or organizations imply endorsement by the U.S. Government.

References

Brennan, R. G., & Sundaralingam, M. (1985) *J. Mol. Biol. 181*, 561–563.

Brennan, R. G., Westof, E., & Sundaralingam, M. (1986) *J. Biomol. Struct. Dyn. 3*, 649–665.

Brunger, A. T. (1988) *J. Mol. Biol. 203*, 803–816.

Calladine, C. R. (1982) *J. Mol. Biol. 161*, 343–352.

Chevrier, B., Dock, A. C., Hartmann, B., Leng, M., Moras, D., Thuong, M. T., & Westhof, E. (1986) *J. Mol. Biol. 190*, 707–719.

Crawford, J. L., Kolpak, F. J., Wang, A. H.-J., Quigley, G. J., van Boom, J. H., van der Marel, G., & Rich, A. (1980) *Proc. Natl. Acad. Sci. U.S.A. 77*, 4016–4020.

Drew, H., Takano, T., Tanaka, S., Itakura, K., & Dickerson, R. E. (1980) *Nature 286*, 567–573.

Fitzgerald, P. M. D. (1988) *J. Appl. Crystallogr. 21*, 273–278.

Felsenfeld, G., & Miles, H. T. (1967) *Annu. Rev. Biochem. 31*, 407–448.

Fishel, R., Derbyshire, M., Dowjat, K., Harris, C. J., & Moore, S. P. (1990) in *Molecular Mechanisms in DNA Replication and Recombination*, pp 343–356, Alan R. Liss, Inc., New York.

Fujii, S., Wang, A. H.-J., van der Marel, G., van Boom, J. H., & Rich, A. (1982) *Nucleic Acids Res. 10*, 7879–7892.

Fujii, S., Wang, A. H.-J., Quigley, G. J., Westerink, H., van der Marel, G., van Boom, J. H., & Rich, A. (1985) *Biopolymers 24*, 243–250.

Gessner, R. V., Frederick, C. A., Quigley, G. J., Rich, A., & Wang, A. H.-J. (1989) *J. Biol. Chem. 264*, 7921–7935.

Hall, K., Cruz, P., & Chamberlin, M. J. (1985) *Arch. Biochem. Biophys. 236*, 47–51.

Harrison, R. W. (1989) *Acta Crystallogr. A45*, 4–10.

Harrison, R. W. (1990) *Acta Crystallogr. A46*, 606–619.

Howard, A. J., Nirlsen, C., & Xuong-Ng, H. (1985) *Methods Enzymol. 114*, 452–472.

Jain, S., & Sundarlingam, M. (1989) *J. Biol. Chem. 264*, 12780–12784.

Jones, T. A. (1985) *Methods Enzymol. 115*, 157–171.

Kennard, O. (1988) in *Structure and Expression* (Sarma, R. H., & Sarma, M. H., Eds.) Vol. 2, pp 1–25, Academic Press, New York.

Leslie, A. G. W., Arnott, S., Chandrasekaran, R., & Ratliff, R. L. (1980) *J. Mol. Biol. 143*, 49–72.

Levitt, M., & Warshell, A. (1978) *J. Am. Chem. Soc. 100*, 2607–2613.

Martin, F. H., Castro, M. M., Aboul-ela, F., & Tinoco, I., Jr., (1985) *Nucleic Acids Res. 13*, 8927–8938.

Miller, M., Harrison, R. W., Wlodawer, A., Appella, E., & Sussman, J. L. S. (1988) *Nature 334*, 85–86.

Mitsui, Y., Langridge, R., Shortle, B. E., Cantor, C. R., Grant, R. C., Kodama, M., & Wells, R. D. (1970) *Nature 228*, 1166–1169.

Pohl, F. M., & Jovin, T. M. (1972) *J. Mol. Biol. 67*, 357–396.

Takahashi, Y., Kato, K., Hayashizaki, Y., Wakabayashi, T., Ohtsuka, E., Matsuki, S., Ikehara, M., & Matsubara, K. (1985) *Proc. Natl. Acad. Sci. U.S.A. 82*, 1931–1935.

Wang, A. H.-J., & Rich, A. (1985) in *Biological Macromolecules and Assemblies, Vol. 2: Nucleic Acids and In-*

teractive Proteins (Jurnak, F. A., & McPherson., A., Eds.) pp 127–170, John Wiley & Sons, New York.
Wang, A. H.-J., Quigley, G. J., Kolpak, F. J., Crawford, J. L., van Boom, J. H., van der Marel, G., & Rich, A. (1979) *Nature 282*, 680–686.
Wang, A. H.-J., Quigley, G. J., Kolpak, F. J., van der Marel, G., van Boom, J. H., & Rich, A. (1981) *Science 211*, 171–176.
Westhoff, E., Dumas, P., & Moras, D. (1985) *J. Mol. Biol. 184*, 119–145.

Hexagonal Phase Forming Propensity Detected in Phospholipid Bilayers with Fluorescent Probes†

Richard M. Epand* and Bryan T.-C. Leon

Department of Biochemistry, McMaster University Health Sciences Centre, 1200 Main Street West, Hamilton, Ontario, Canada L8N 3Z5

Received September 5, 1991; Revised Manuscript Received November 1, 1991

ABSTRACT: The fluorescence emission spectrum of N^{ϵ}-dansyl-L-Lys undergoes a marked blue shift when incorporated from aqueous solution into phospholipid bilayers. This shift is greater for membranes composed of dipalmitoleoylphosphatidylcholine than for membranes of dipalmitoleoylphosphatidylethanolamine. With the latter but not the former lipid, the fluorescence emission from N^{ϵ}-dansyl-L-Lys is markedly temperature-dependent. The marked temperature dependence of N^{ϵ}-dansyl-L-Lys fluorescence in bilayers of dipalmitoleoylphosphatidylethanolamine is greatest as the sample is heated close to the bilayer to hexagonal phase transition temperature. The fluorescence emission properties of another probe of membrane surface hydrophobicity, Laurdan, also exhibit marked changes at temperatures just below the bilayer to hexagonal phase transition temperature. At these temperatures, the generalized polarization begins to increase rather than decrease with temperature, and the emission intensity decreases markedly. Such effects are not observed over the same temperature range with phosphatidylcholine. Thus, both dansyl-L-lysine and Laurdan provide probes to measure changes in the physical properties of membrane bilayers which occur when these bilayers are heated close to the temperature required for transition to the hexagonal phase.

The rearrangement of lipid bilayers to morphologically distinct forms has been recognized for many years (Luzzati, 1968). Much attention was given to the possible biological functions of nonbilayer phases (Cullis & deKruijff, 1979). Although some evidence indicates the presence of the nonbilayer inverted hexagonal (H_{II}) phase in biological membranes, the presence of such structures in cell membranes has still not yet been conclusively proven. It is clear that, even if present, the H_{II} phase is not a common or prevalent feature of biological membranes. More recent studies have indicated that the H_{II} itself may not be required for biological function. For example, fusion of phospholipid vesicles does not require the formation of H_{II} phases (Ellens et al., 1989). Nevertheless, bilayer membranes which are more prone to undergo conversion to the H_{II} phase are also more prone to undergo membrane fusion or to promote the activity of certain membrane-bound enzymes (Yeagle, 1989; Hui & Sen, 1989; Epand, 1990). The propensity of a membrane to form the H_{II} phase has been judged by measuring the temperature at which there is a cooperative transition from the bilayer (L_{α}) to the H_{II} phase. However, if shifts in this phase transition temperature are correlated with alterations of the functional properties of bilayer membranes, then the physical properties of the bilayer phase itself must be altered. It is difficult to directly measure changes in the physical properties of the bilayer phase which result from changes in the tendency of each monolayer of the bilayer to curve (Gruner, 1985). This is because these changes in the intrinsic radius of curvature of each monolayer are not expressed as a change in lipid morphology while the membrane is constrained to form a planar bilayer. In the present study, we demonstrate that differences in properties among membrane bilayers can be detected by fluorescence using the probes N^{ϵ}-[5-(dimethylamino)naphthalene-1-sulfonyl]-L-lysine (DNS-Lys)[1] or Laurdan. These properties of the bilayer which affect the fluorescence properties of these probes are correlated with the tendency of the bilayer to form the H_{II} phase.

The fluorescence emission from the dansyl chromophore is known to be very sensitive to the solvent environment. Two types of dansyl derivatives have been used to probe membrane properties. They are dansylated phospholipids (Kimura & Ikegami, 1985; Ohki & Arnold, 1990) and dansylated amino acids. The dansyl group attached to the phospholipid headgroup is relatively fixed in position at the surface of the bilayer, while the dansyl group of dansylated amino acids can intercalate to various depths near the bilayer surface. The fluorescence emission of dansylglycine is particularly sensitive to lipid packing in that it can detect differences between the inner and outer monolayers of small lipid vesicles (Bramhall, 1986). This fluorescent molecule also detects changes in lipid

† Supported by Medical Research Council of Canada Grant MA7654.

[1] Abbreviations: DNS-Lys, N^{ϵ}-[5-(dimethylamino)naphthalene-1-sulfonyl]-L-lysine or dansyl-L-lysine; Laurdan, 6-dodecanoyl-2-(dimethylamino)naphthalene; DiPoPE, L-α-dipalmitoleoylphosphatidylethanolamine; DiPoPC, L-α-dipalmitoleoylphosphatidylcholine; DSC, differential scanning calorimetry; GP, generalized polarization.

0006-2960/92/0431-1550$03.00/0